



## Fissile fuel breeding with peaceful nuclear explosives

Sümer Şahin<sup>a,\*</sup>, Şenay Yalçın<sup>b</sup>, Kadir Yıldız<sup>c</sup>

<sup>a</sup> *Teknik Eğitim Fakültesi, Gazi Üniversitesi, Beşevler, Ankara 06503, Turkey*

<sup>b</sup> *Fen-Edebiyat Fakültesi, Bahçeşehir Üniversitesi, İstanbul, Turkey*

<sup>c</sup> *Aksaray Mühendislik Fakültesi, Niğde Üniversitesi, Niğde, Turkey*

Received 1 November 2002; accepted 1 May 2003

### Abstract

Neutron physics analysis of a dual purpose modified PACER concept has been conducted. A protective liquid droplet jet zone of 2 m thickness is considered as coolant, energy carrier, and fusile and fissile breeder. Flibe as the main constituent is mixed with increased mole-fractions of heavy metal salt (ThF<sub>4</sub> and UF<sub>4</sub>) starting by 2 up to 12 mol.%. The neutronic model assumed a 30 m radius underground spherical geometry cavity with a 1 cm thick SS-304 stainless steel liner attached to the excavated rock wall. By a self-sufficient tritium breeding of 1.05 with 5 mol.% ThF<sub>4</sub>, or 9 mol.% UF<sub>4</sub> an excess nuclear fuel breeding rate of 1900 kg/year of <sup>233</sup>U or 3000 kg/year <sup>239</sup>Pu of extremely high isotopic purity can be realized. This precious fuel can be considered for special applications, such as spacecraft reactors or other compact reactors. The heavy metal constituents in jet zone acts as an energy amplifier, leading to an energy multiplication of  $M = 1.27$  or  $1.65$  for 5 mol.% ThF<sub>4</sub>, or 9 mol.% UF<sub>4</sub>, respectively. As an immediate result of the strong neutron attenuation in the jet zone, radiation damage with dpa < 1.4 and He < 7 ppm after a plant operation period of 30 years will be well below the damage limit values. The site could essentially be abandoned, or the cavity could be used as a shallow burial site for other qualified materials upon decommissioning. Finally, the totality of the site with all nuclear peripheral sections must be internationally safeguarded carefully.

© 2003 Elsevier B.V. All rights reserved.

*Keywords:* PACER concept; Fissile fuel; Neutron physics

### 1. Introduction

The growing world energy needs require exploring new energy sources. Nuclear fusion has a great potential to provide a cheap, environmentally benign, and inexhaustible energy. At present,

research efforts on fusion energy production are conducted, through two mean lines, namely magnetic fusion energy (MFE) and inertial fusion energy (IFE). However, prognoses indicate that there is a long way until controlled fusion may become economically competitive. On the other hand, the use of nuclear explosives is the only proven and in-hand way to release fusion energy on a usefully macro scale. The idea of producing electricity through peaceful nuclear explosive

\* Corresponding author. Tel.: +90-312-212-4304; fax: +90-312-212-0059.

E-mail address: [sumer@gazi.edu.tr](mailto:sumer@gazi.edu.tr) (S. Şahin).

(PNE) devices has been elaborated gradually since early 1960s. Sound proposals are evaluated for power production by repetitive nuclear explosions contained in an underground cavity [1–9]. One of the most prospective ideas turns out to be the so-called modified PACER concept. The problems concerning chamber design under consideration of the mechanical forces following the explosion, fireball pressure dynamics and equilibrium pressure have been discussed in [6–9].

Preceding calculations have further shown that for a Flibe zone thickness of  $>2.5$  m, the activation of the steel liner and rock would be low enough after 30 years of operation that the cavity would satisfy the US Nuclear Regulatory Commission's rules for "shallow burial" upon decommissioning, assuming other sources of radioactivity could be removed or qualified as well. This implies that upon decommissioning, the site could essentially be abandoned, or the cavity could be used as a shallow burial site for other qualified nuclear waste materials. It is tacitly understood that a power plant site on the basis of nuclear explosives must be constructed in a remote uninhabited area.

The modified PACER concept [7–9] was evaluated for power production, only. However, being a neutron reach source, a fusion power plant can also be used for fissile fuel breeding (FFB). For that reason, the flowing liquid zone will be composed of a mixture of Flibe and fissionable heavy metal salt ( $\text{ThF}_4$  and  $\text{UF}_4$ ) for the purpose of a self-sufficient tritium breeding for the PNE power plant and for FFB for utilization in external light water reactors (LWRs) in the present work.

## 2. The PACER concept

In the modified PACER concept, the layout of the generic power station is shown in Fig. 1, as adopted from [8,9], which was also originally adopted from [10,11]. The parts of such a plant are an underground containment vessel, the explosive with its operating mechanism, the heat-transfer system, the electric generator, the cooling system, the nuclear material reprocessing plant

and the explosive manufacturing plant. A simplified sequence of operations in the power plant is shown in Fig. 2, as adopted from [9].

The explosion yield is 2 kt (8.36 TJ) every 40 min in a 20 m radius cylindrical cavity, carefully engineered with a 1-cm-thick stainless steel liner. The liner is secured to the rock with regularly spaced and pre-stressed rock bolts or tendons. These measures lead to a reasonably reduced the cavity volume [6,7]. The steel skin is convex to keep it tightly stretched against the rock, as shown in Fig. 3, adopted from [6]. The liner prevents a contamination of the molten salt with rock material and reinforces the rock media. Liquid jets or streams surround the explosion in order to reduce the mechanical forces on the steel liner from the dynamic stresses caused by the shocks from the explosion. An alternative way for shock suppression system using springs and shock absorbers behind plates is presented in [12]. However, liquid jets have the fundamental advantage of the instantaneous recovery. In this concept, the working fluid is molten salt,  $\text{Li}_2\text{BeF}_4$  (Flibe), in the form of vertically flowing jets, to absorb energy and protect the liner from shocks. This allows much of the energy to evaporate the liquid and keeps a reduced pressure  $\sim 3$  MPa in the cavity right after the explosion. Also, because tritium is practically insoluble in the molten salt, it can be removed almost completely, thus allowing a very low tritium inventory in the range of  $\sim 100$  Ci by using Flibe [6].

In the present work, while Flibe remains as the main constituent of vertically flowing jets, now it is mixed with increased mole-fractions of heavy metal salt ( $\text{ThF}_4$  and  $\text{UF}_4$ ), starting by 2 up to 12 mol.%, for the purpose of high quality FFB, under consideration of a self-sufficient tritium breeding for the PNE fusion device. High quality fissile fuel will be needed primarily for the igniter of the PNE device. Excess fissile fuel can be used for external spacecraft reactors or other advanced reactor systems. Actual LWRs are operating with low enriched nuclear fuel so that high quality fissile fuel could be utilized more economical in compact reactors for special missions.

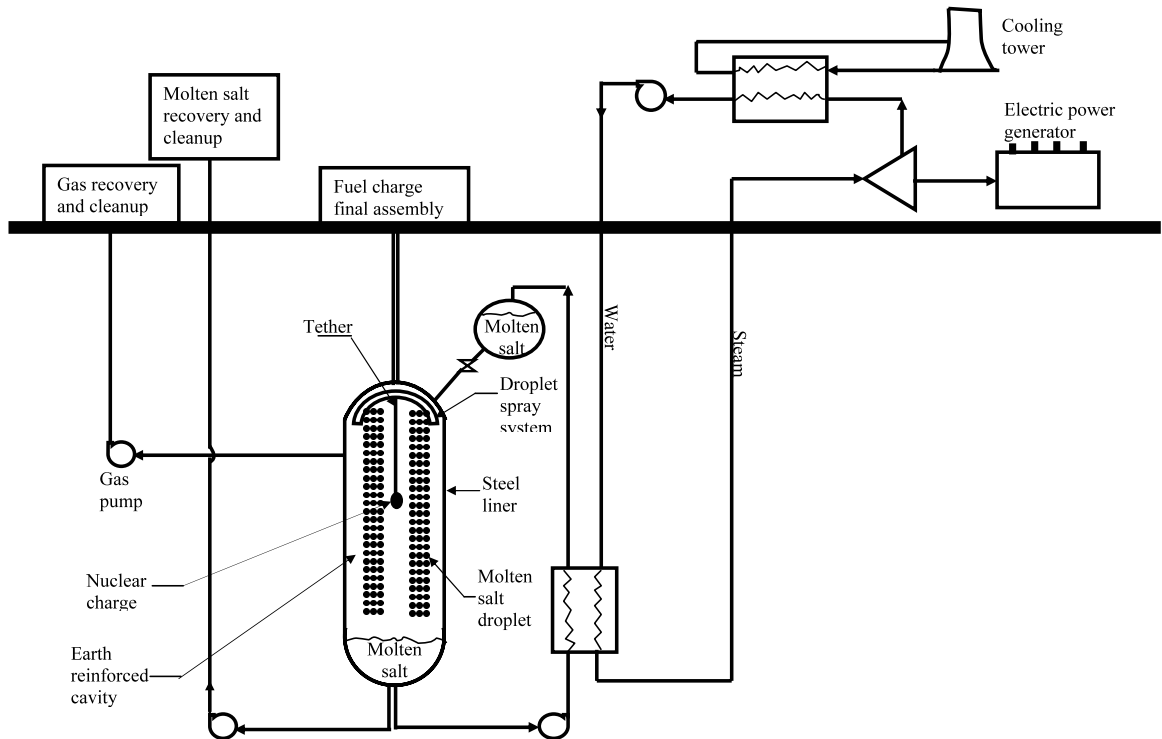


Fig. 1. Schematic diagram of a PNE reactor power station. The diagram identifies its principal components (adopted from [8,9]).

### 3. Calculation procedure

In the course of the numerical analysis, the cylindrical cavity was simulated by a spherical one. This substitution allowed us to perform a series of fast, one-dimensional multi-group neutron transport calculations with a sufficiently high resolution in the neutron energies of interest. The neutron source is evaluated, based on a fusion nuclear explosive device.

#### 3.1. Geometrical model for neutronic calculations

A rigorous neutronic study at advanced design stage would require three-dimensional calculation tools. However, for the purpose of a generic study with fast, multiple computer runs, one-dimensional calculations will be preferred, for simplicity. Any type of a fusion blanket must cover the neutron source over a space angle of  $4\pi$  to confine the fusion neutrons, among other reasons. One-

dimensional slab or cylinder would represent open geometries. Therefore, calculations are conducted in this and related previous work, preferably in one-dimensional spherical geometry under consideration of the neutron spectrum softening due to neutron backscattering into the cavity in a closed geometry [13–17].

Fig. 4 shows the neutronic calculation model of the cavity. The space, where the PNE device is located in a spherical cavity with a radius of  $R = 5$  m. The molten salt zone consisting of liquid jets has a radial thickness of  $DR = 2.0$  m. The basic constituent of molten salt is Flibe. Previous work has shown that a Flibe jets zone of  $DR > \sim 2$  m would reduce the residual reactivity to such low levels that the 10CFR61 regulations [18] can be satisfied for a C-class nuclear waste disposal after decommissioning [13–17]. In the present work, heavy metal in form of  $\text{ThF}_4$  or  $\text{UF}_4$  has been added to Flibe for the purpose of FFB. The molecular fraction of the latter component is

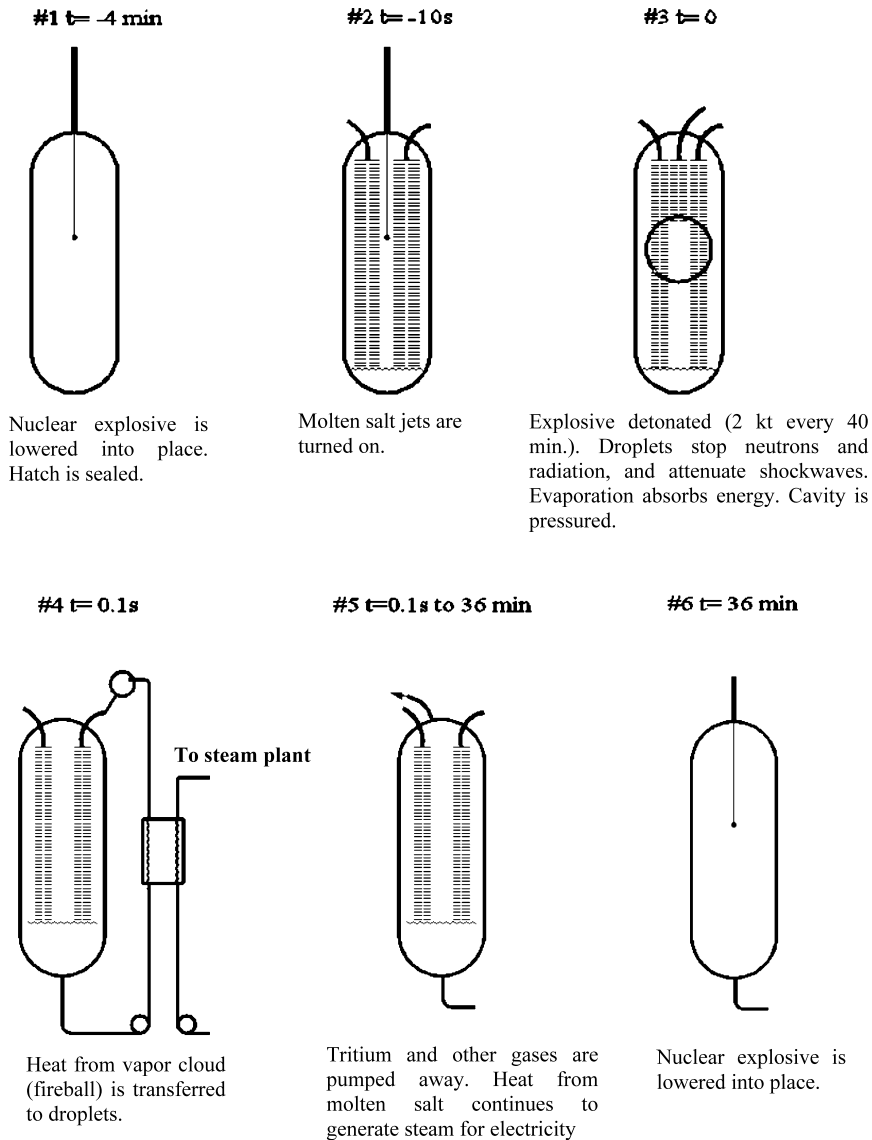


Fig. 2. Sequence of events in the operation of a PNE reactor (adopted from [9]).

gradually increased from 2 up to 12% in the coolant. The cavity is lined with 1 cm-thick stainless steel of type SS-304. Steel structures can be made of SS-304 steel rather than of SS-316 due to the lack of corrosive water in the cavity in order to satisfy the 10CFR61 regulations with more safety margin. Beyond the liner, a 50-cm rock zone is used to consider the neutron reflection back into the cavity. For  $DR > 50 \text{ cm}$ , the

neutrons reaching the rock zone could act practically infinite with respect to neutron reflection.

Table 1 shows the atomic densities of the materials, as used in the calculations. The atomic densities for rock around the cavity were adopted to correspond to the average values in the Nevada region [19]. We assumed the neutron source to be entirely 14 MeV, as the authors are not interested in nuclear weapon design.

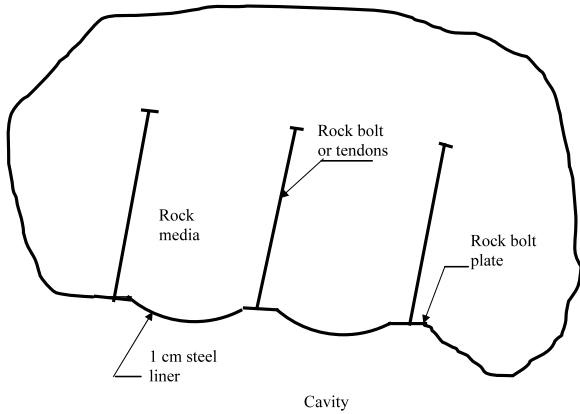


Fig. 3. The convex-shaped-skin cavity liner is attached to the rock material with rock bolts (adopted from [6]).

### 3.2. Computational tools

Neutron transport calculations are conducted in spherical geometry with the help of SCALE4.4A SYSTEM by solving the Boltzmann transport equation with code XSDRNPM [20] in  $S_8-P_3$  approx-

imation with Gaussian quadratures [21] using the 238 groups library [22], derived from ENDF/B-V. The resonance calculations in the fissionable fuel element cell are performed with

- BONAMI [23] for unresolved resonances, and
- NITAWL-II [24] for resolved resonances.

CSAS control module [25] is used to produce the resonance self-shielded weighted cross-sections for XSDRNPM.

### 4. Numerical results

The objective of this work is to investigate primarily the possibilities for a totally self-sustained nuclear fuel supply of the PNE power plant with respect to tritium needs for the main PNE device and also to high quality fissile fuel needs for the igniter. In the course of calculations, the tritium and fissile fuel production, total nuclear heat release, neutron radiation damage on the liner

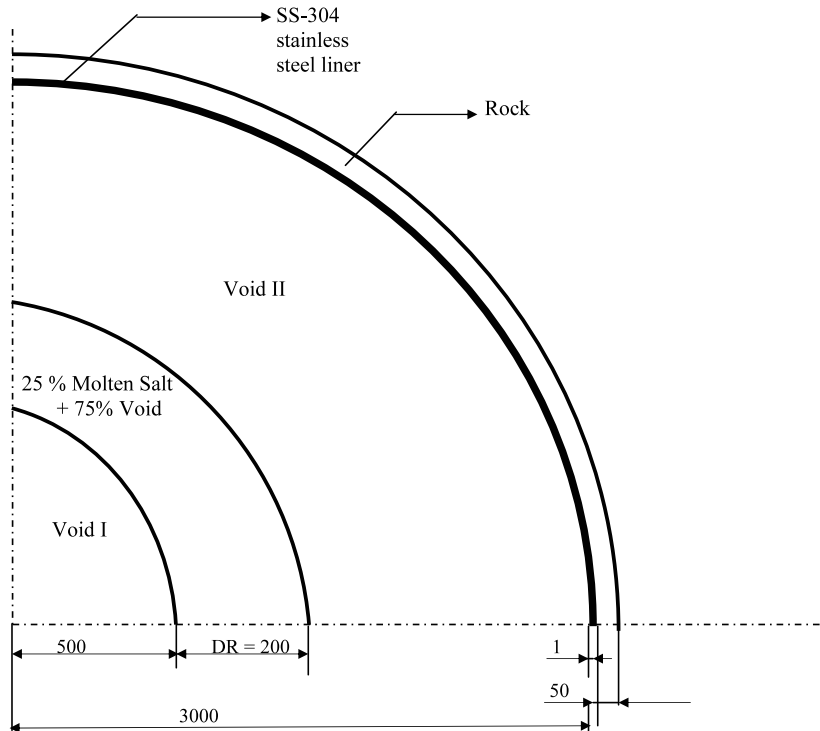


Fig. 4. Neutronic calculation model of PNE reactor cavity (dimension are given in cm).

Table 1  
Atomic densities of the materials, as used in the calculations

Material	Nuclide	Nuclei density ( $10^{24}/\text{cm}^3$ )
Molten salt $(\text{UF}_4)_{0.02} \cdot (\text{Li}_2\text{BeF}_4)_{0.98}$	$^{238}\text{U}$	$5.98835\text{E-}05^{\text{a}}$
	$^{235}\text{U}$	$4.22139\text{E-}07$
	$^{19}\text{F}$	$1.20611\text{E-}02$
	$^9\text{Be}$	$2.95497\text{E-}03$
	$^7\text{Li}$	$5.46670\text{E-}04$
	$^6\text{Li}$	$4.43246\text{E-}04$
Molten salt $(\text{UF}_4)_{0.04} \cdot (\text{Li}_2\text{BeF}_4)_{0.96}$	$^{238}\text{U}$	$1.19917\text{E-}04$
	$^{235}\text{U}$	$8.45340\text{E-}07$
	$^{19}\text{F}$	$1.20763\text{E-}02$
	$^9\text{Be}$	$2.89831\text{E-}03$
	$^7\text{Li}$	$5.36187\text{E-}03$
	$^6\text{Li}$	$4.34746\text{E-}04$
Molten salt $(\text{UF}_4)_{0.06} \cdot (\text{Li}_2\text{BeF}_4)_{0.94}$	$^{238}\text{U}$	$1.80103\text{E-}04$
	$^{235}\text{U}$	$1.26961\text{E-}06$
	$^{19}\text{F}$	$1.20915\text{E-}02$
	$^9\text{Be}$	$2.84150\text{E-}03$
	$^7\text{Li}$	$5.25677\text{E-}03$
	$^6\text{Li}$	$4.26225\text{E-}04$
Molten salt $(\text{UF}_4)_{0.08} \cdot (\text{Li}_2\text{BeF}_4)_{0.92}$	$^{238}\text{U}$	$2.40439\text{E-}04$
	$^{235}\text{U}$	$1.69494\text{E-}06$
	$^{19}\text{F}$	$1.21067\text{E-}02$
	$^9\text{Be}$	$2.78454\text{E-}03$
	$^7\text{Li}$	$5.15141\text{E-}03$
	$^6\text{Li}$	$4.17682\text{E-}04$
Molten salt $(\text{UF}_4)_{0.10} \cdot (\text{Li}_2\text{BeF}_4)_{0.90}$	$^{238}\text{U}$	$3.00928\text{E-}04$
	$^{235}\text{U}$	$2.12135\text{E-}06$
	$^{19}\text{F}$	$1.21220\text{E-}02$
	$^9\text{Be}$	$2.72745\text{E-}03$
	$^7\text{Li}$	$5.04578\text{E-}03$
	$^6\text{Li}$	$4.09117\text{E-}04$
Molten salt $(\text{UF}_4)_{0.12} \cdot (\text{Li}_2\text{BeF}_4)_{0.88}$	$^{238}\text{U}$	$3.61570\text{E-}04$
	$^{235}\text{U}$	$2.54883\text{E-}06$
	$^{19}\text{F}$	$1.21373\text{E-}02$
	$^9\text{Be}$	$2.67021\text{E-}03$
	$^7\text{Li}$	$4.93988\text{E-}03$
	$^6\text{Li}$	$4.00531\text{E-}04$
Molten salt $(\text{ThF}_4)_{0.02} \cdot (\text{Li}_2\text{BeF}_4)_{0.98}$	$^{232}\text{Th}$	$6.02221\text{E-}05$
	$^{19}\text{F}$	$1.20444\text{E-}02$
	$^9\text{Be}$	$2.95088\text{E-}03$
	$^7\text{Li}$	$5.45914\text{E-}03$
	$^6\text{Li}$	$4.42633\text{E-}04$
	$^{232}\text{Th}$	$1.20429\text{E-}04$
Molten salt $(\text{ThF}_4)_{0.04} \cdot (\text{Li}_2\text{BeF}_4)_{0.96}$	$^{19}\text{F}$	$1.20429\text{E-}02$
	$^9\text{Be}$	$2.89028\text{E-}03$
	$^7\text{Li}$	$5.34703\text{E-}03$
	$^6\text{Li}$	$4.33543\text{E-}04$
	$^{232}\text{Th}$	$1.80619\text{E-}04$
	$^{19}\text{F}$	$1.20413\text{E-}02$
Molten salt $(\text{ThF}_4)_{0.06} \cdot (\text{Li}_2\text{BeF}_4)_{0.94}$	$^9\text{Be}$	$2.82970\text{E-}03$
	$^7\text{Li}$	$5.23495\text{E-}03$
	$^6\text{Li}$	$4.24455\text{E-}04$

Table 1 (Continued)

Material	Nuclide	Nuclei density ( $10^{24}/\text{cm}^3$ )
Molten salt $(\text{ThF}_4)_{0.08} \cdot (\text{Li}_2\text{BeF}_4)_{0.92}$	$^{232}\text{Th}$	$2.40794\text{E-}04$
	$^{19}\text{F}$	$1.20397\text{E-}02$
	$^9\text{Be}$	$2.76913\text{E-}03$
	$^7\text{Li}$	$5.12289\text{E-}03$
	$^6\text{Li}$	$4.15370\text{E-}04$
Molten salt $(\text{ThF}_4)_{0.10} \cdot (\text{Li}_2\text{BeF}_4)_{0.90}$	$^{232}\text{Th}$	$3.00953\text{E-}04$
	$^{19}\text{F}$	$1.20381\text{E-}02$
	$^9\text{Be}$	$2.70858\text{E-}03$
	$^7\text{Li}$	$5.01087\text{E-}03$
	$^6\text{Li}$	$4.06287\text{E-}04$
Molten salt $(\text{ThF}_4)_{0.12} \cdot (\text{Li}_2\text{BeF}_4)_{0.88}$	$^{232}\text{Th}$	$3.61097\text{E-}04$
	$^{19}\text{F}$	$1.20366\text{E-}02$
	$^9\text{Be}$	$2.64804\text{E-}03$
	$^7\text{Li}$	$4.89888\text{E-}03$
	$^6\text{Li}$	$3.61097\text{E-}04$
SS-304	C	$1.47870\text{E-}05$
	Fe	$6.01898\text{E-}02$
	Ni	$8.59854\text{E-}03$
	Si	$3.43942\text{E-}04$
	Cr	$1.63372\text{E-}02$
	Rock (Nevada $\rho = 1.63 \text{ g/cm}^3$ ) [18]	H
	O	$3.57300\text{E-}02$
	Mg	$4.90100\text{E-}04$
	Na	$4.45200\text{E-}04$
	Al	$4.50800\text{E-}04$
	Fe	$3.42700\text{E-}04$
	Si	$1.16400\text{E-}04$

<sup>a</sup> Read as  $5.98835 \times 10^{-5}$ .

are evaluated. Excess fissile fuel production for the external use will also be calculated. In the first step, neutron spectrum in the cavity has been evaluated.

#### 4.1. Neutron spectrum

We assumed the neutron source to be entirely 14 MeV. In previous work, an attempt to assess the correct neutron leakage spectrum out of a PNE has shown that this would not be reliable without an exact knowledge of the geometry and material composition of the explosive [26]. As the authors are not interested in nuclear weapon design, we also assumed that any material surrounding the neutron source could be considered equivalently to be internal part of the molten salt zone with respect to spectral displacements. In a reflection with inertial confined fusion (ICF), we remember

that an ICF target has a  $1000 \times$  of liquid density. Whereas, a fusion zone of a PNE will have at most  $20\text{--}50 \times$  of liquid density.

With that assumption in mind, transport calculations are conducted to evaluate the space- and energy dependent neutron spectrum in the cavity. As one can see in Fig. 4, the 14 MeV energetic fusion source neutrons arrive, practically unhindered through the first void, to the liquid jet region. Majority of neutron interactions takes place in the molten salt coolant and shape the neutron spectrum. Then, again the leaking neutrons pass the second void region and penetrate through the liner into the rock. Further neutron interactions occur in the rock. Neutron spectrum in the coolant determines all pertinent neutron reaction rates, and has hence primary importance.

Calculations have shown that the increase of heavy metal along with the decrease of lithium has compensating effects on neutron absorption with very minor effects on the spectrum, keeping the latter practically unchanged for the investigated coolant compositions. Addition of the heavy to the coolant increases slightly the induced fission neutron part in the spectrum. Flibe has dominating effects on the spectrum formation due to the light elements, such as Be and Li.

Fig. 5 shows the neutron spectrum by deep penetration through the molten salt with 12 mol.% heavy metal. Spectrum consists of the uncollided fusion source neutrons, collided neutrons and secondary fission neutrons. Strong resonance depths are noticed with the presence of  $\text{UF}_4$ . Towards the right border of the jet zone, a remarkable neutron thermalization throughout the coolant region is observed resulting with a typical Maxwellian shape in thermal energies.

Neutrons will be multiplied in the coolant via fission and  $(n, 2n)$  in the coolant. To some degree, also  $(n, 3n)$  reactions will occur in the heavy metal. Although a great fraction of neutrons will also be absorbed in situ, some neutrons will leak out of the coolant. Right neutron leakage fraction out of coolant towards the liner increases very slightly from 12.4 to 12.7% for 2 to 12 mol.%  $\text{UF}_4$  fraction, respectively, and decreases very slightly from 12.3 to 11.9% for 2–12 mol.%  $\text{ThF}_4$  fraction, respectively. The higher neutron multiplication in

$\text{UF}_4$  causes this very slight increase of right neutron leakage fraction despite a stronger neutron absorption in natural uranium.

#### 4.2. Fusile fuel (tritium) breeding

Like every fusion reactor concept, also a PNE power plant must produce its own artificial and radioactive fusile fuel tritium in the course of operation for a self-sustained fusion fuel supply. For that reason a tritium breeding ratio (TBR)  $> 1.05$  can be considered satisfactory. In recent work, an extensive neutronic analysis of the modified PACER concept has been carried out [27]. Using  $\text{Li}_2\text{BeF}_4$  as the working fluid in form of vertically flowing jets with a volume fraction of 25%, Flibe zone thickness of 1.6 and 2 m were evaluated for a TBR value of 1.05 and 1.15, respectively. In the present work, by a liquid zone thickness of 2.0 m, lithium is gradually replaced with heavy metal for the purpose of fissile breeding. Along with the increase of the heavy metal fraction in the jets, fusile breeding rates will decline and fissile breeding rates will grow in adverse sense.

Fig. 6 depicts the TBR as a function of the heavy metal fraction in the coolant. While the  $T_7$  value (TBR in  ${}^7\text{Li}$ ) remains the same for both  $\text{UF}_4$  and  $\text{ThF}_4$ , and furthermore practically unchanged over a long fraction range,  $T_6$  value (TBR in  ${}^6\text{Li}$ ) drops along with increasing heavy metal fraction. Also, higher neutron multiplication in natural uranium than in thorium leads to a higher production for low energy neutrons, resulting in higher neutron absorption in  ${}^6\text{Li}$  and consequently with higher  $T_6$ , in the former.

According to the total TBR values in Fig. 6, Flibe coolant with up to 5 mol.%  $\text{ThF}_4$  or with up to 9 mol.%  $\text{UF}_4$  will allow a self-sufficient tritium breeding by a thickness of 2 m. Previous work has indicated that the TBR increases according to the fitted analytical relation  $\text{TBR} = A \tanh(b \cdot \text{DR})^c$  with increasing coolant zone thickness DR, and reaches soon beyond  $> 2$  m an asymptote [27]. Of course, with U and Th fluorides in the Flibe jets, the constants in the analytical relation will be slightly different, but the shape of the analytical function will have, more or less, a similar character.

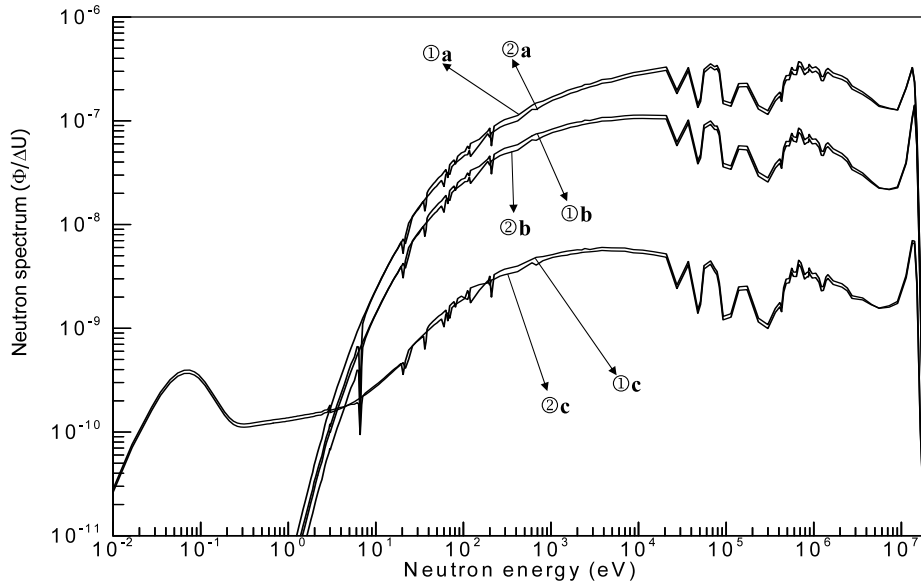


Fig. 5. The neutron spectrum through the molten salt with 12 mol.% heavy metal content: (1): with  $\text{UF}_4$ ; (2): with  $\text{ThF}_4$ ; a: at the left side; b: in the middle; c: at the right side of molten salt region.

#### 4.3. Fissile fuel breeding

Heavy metal in the coolant has a dual function. Through neutron capture and fission, it serves for FFB and energy multiplication, respectively. Tritium breeding and FFB growth in opposite direc-

tions by variation of heavy metal content in the coolant. As the residence time of the intermediate actinide isotope ( $^{233}\text{Pa}$  or  $^{239}\text{Np}$ ) under neutron irradiation will be as long as the explosion pulse length, hence extremely short ( $< \mu\text{s}$ ), and furthermore the irradiated coolant will be removed after

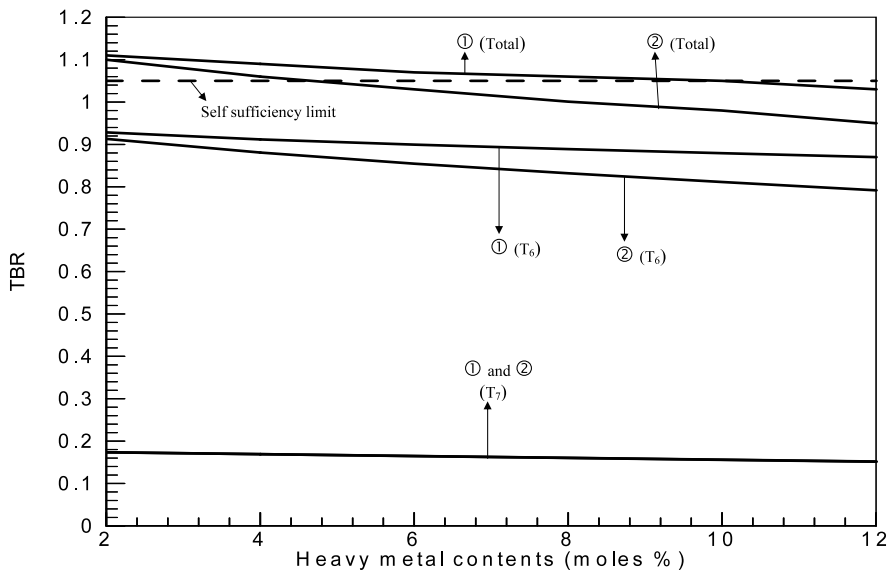


Fig. 6. Tritium production in the blanket: (1): with  $\text{UF}_4$ ; (2): with  $\text{ThF}_4$ .



each explosion out of the reactor cavity, the newly produced fissile fuel will be of extreme isotopic purity, never attainable in conventional reactors. For that reason, it would be, to a certain degree, a waste to use this high quality fuel in standard nuclear reactors. It would be rather predestinated for new application fields, such as space craft or other types of compact reactors.

Some of the fissile fuel can be utilized for the fission trigger of the PNE device, which can be roughly estimated. In a well developed PNE device, most of the explosion energy must be supplied by fusion. We assume that the fission trigger can be designed as compact as possible so that by a well developed compression technique its explosion energy will be  $\sim 10\%$  of the fusion component, namely  $\sim 0.2$  kT/shot. For that energy release, the fissile fuel consumption will be  $\sim 10$  g/shot or  $\sim 130$  kg/year. The rest of the fissile fuel (unburnt fraction) in the PNE device will be mixed with the coolant together with other explosion debris and can be recuperated along with the new fissile fuel in the coolant. Fig. 7 shows the gross (total) FFB/year and the net fissile fuel production for external use by a repetition rate of 40 min/shot for a full power year.

#### 4.4. Nuclear energy generation

In addition to the fusion explosion energy of the PNE device, there will be some additional nuclear energy production in the molten jet zone. The 238 group's library in the SCALE4.4A SYSTEM contains only neutron energy groups and not the  $\gamma$ -rays. Heat production data with inclusion of all nuclear reactions are not processed in this cross section set. Within the framework of the present work and for the purpose of an assessment of nuclear heating in the coolant, neutron induced fission reactions in heavy metal and the main energetic reactions in lithium, namely  ${}^6\text{Li}(n, \alpha)\text{T}$  and  ${}^7\text{Li}(n, \alpha n')\text{T}$  reactions have been considered, as in equation (1), which constitute major components of nuclear power production.

$$E = \langle \Sigma_f \Phi \rangle 180 \text{ MeV} + \langle T_6 \rangle 4.784 \text{ MeV} - \langle T_7 \rangle 2.467 \text{ MeV} \quad (1)$$

Natural uranium and thorium become fissionable under high energetic fusion neutron irradiation, and produce power. Fig. 8 depicts the integral fission rate in the coolant per incident fusion neutron as a function of heavy metal content in the coolant. Natural uranium is to a higher degree fissionable than thorium. Integral fission in  $\text{UF}_4$  and  $\text{ThF}_4$  increases by a factor of 5 and 4.9, respectively, for an increase of heavy metal from 2 to 12% in the coolant. Despite this relative increase, total integral fission rate remains very low, namely only a few% with  $\text{UF}_4$  and  $< 1\%$  with  $\text{ThF}_4$  leading to only a modest and minor energy multiplication, respectively, in the PNE power plant system. Main energy source in the modified PACER system with fissionable remain the PNE device.

Fig. 9 shows the total energy multiplication factor  $M$  in the PNE reactor. With  $\text{UF}_4$  in the coolant,  $M$  increases by 35% from 2 to 12% heavy metal in the coolant. On the other hand,  $M$  increases by only 6.6% from 2 to 12% thorium in the coolant. The energy production in  ${}^6\text{Li}$  and in thorium remains nearly comparable so that the depletion in  ${}^6\text{Li}$  is barely compensated by replacement with thorium. Therefore, the contribution of  $\text{ThF}_4$  to energy multiplication becomes almost negligible. Under consideration of a self-sufficient tritium breeding ( $\text{TBR} > 1.05$ ), the upper limits are 5 mol.% for  $\text{ThF}_4$  and 9 mol.% for  $\text{UF}_4$ , Section 4.2. Then, the upper energy multiplication values will be  $M = 1.27$  for 5 mol.%  $\text{ThF}_4$ , and 1.65 for 9 mol.%  $\text{UF}_4$ .

Total nuclear heat production will consists of (1) the explosion energy of the PNE device and (2) the instantaneous, isochoric, neutron induced heat release in the coolant. Fig. 10 shows the induced nuclear heat density in the coolant zone as a function of the distance from the neutron source. The instantaneous energy generation density at the time of explosion is very high. Fission has an exponentially decreasing character with increasing distance from the neutron source due to a relatively high threshold fission energy in  ${}^{232}\text{Th}$  (1.4 MeV) and  ${}^{238}\text{U}$  (0.8 MeV). On the other hand, the exothermic  ${}^6\text{Li}(n, \alpha)$  reactions are dominated by low energy secondary neutrons and have a cosine like flat character.

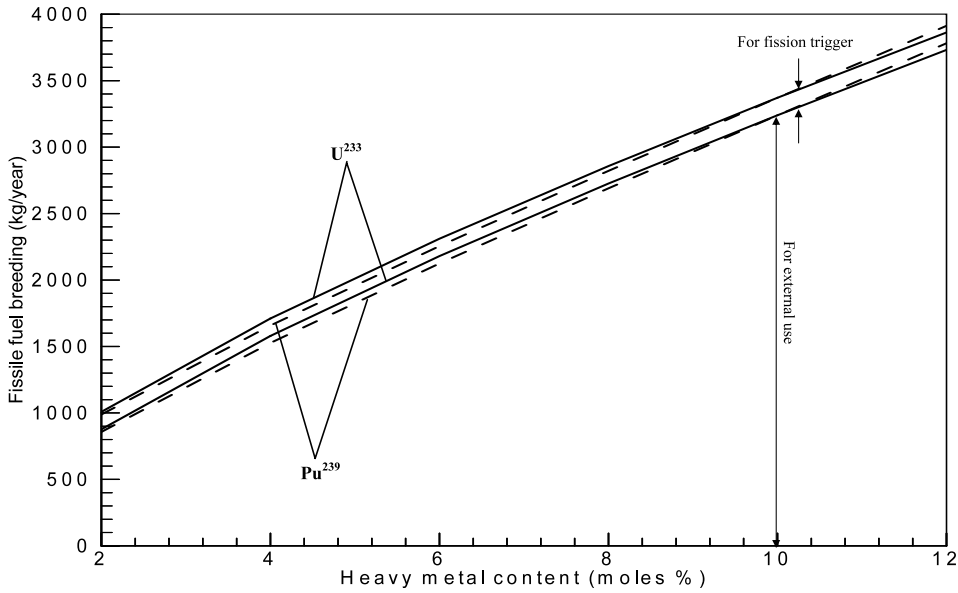


Fig. 7. FFB per incident fusion neutron.

Explosion and the induced nuclear energy will create a fireball and the total energy produced will be transferred to the stream of droplets. Jets will continue to cool vapor. Temperature and pressure will drop to 1500 K and 1 atm in 0.1 s. The explosion will mix up all the coolant in the

chamber and very quickly an almost homogenous and isothermal coolant will be accumulated at the bottom, indicated in Fig. 2. Molten salt will then be pumped to heat exchanger.

Contribution of  $\gamma$ -rays to total nuclear heat is discussed in Section 4.5.

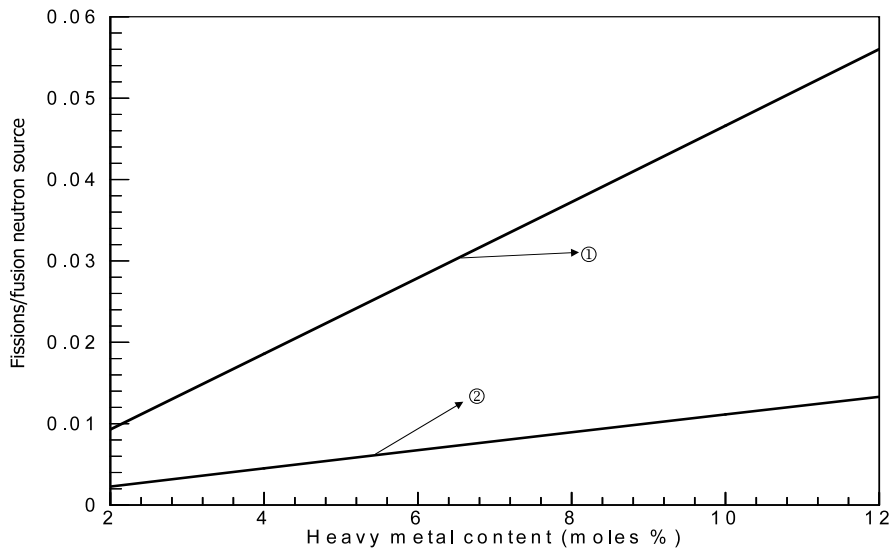


Fig. 8. The integral fission rate in the coolant per incident fusion neutron as a function of heavy metal content in the coolant: (1): with UF<sub>4</sub>; (2): with ThF<sub>4</sub>.

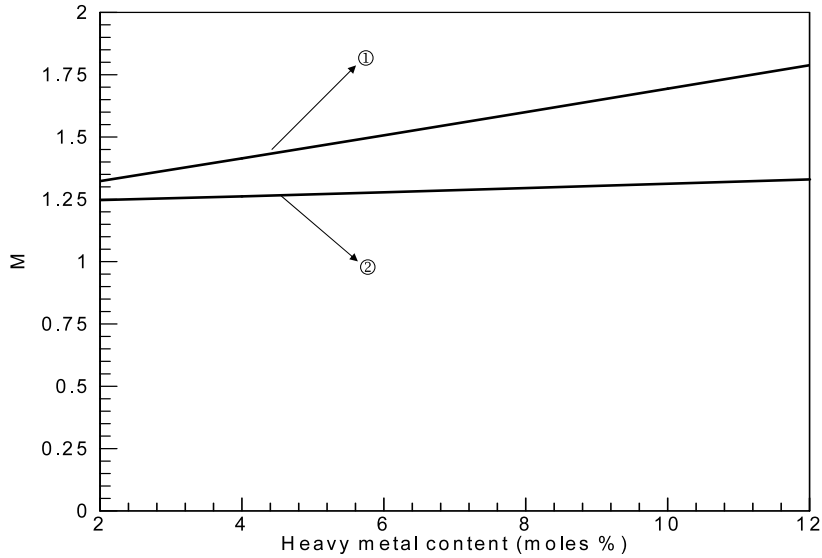


Fig. 9. The total energy multiplication factor  $M$  in the PNE reactor: (1): with  $UF_4$ ; (2): with  $ThF_4$ .

#### 4.5. Contribution of $\gamma$ -rays to nuclear heat

In Section 4.4, the nuclear power production is analyzed with the help of the 238 neutron group library in a fine energy resolution and under consideration of resonance effects for each problem, individually. Previous work had demonstrated clearly the importance of a fine neutron energy resolution and consideration of resonance effects for fusion blanket neutronic studies [27]. However, the heat production data considering all nuclear reactions are not processed in the 238 group cross sections set [22]. For an assessment of the contribution of  $\gamma$ -rays on total nuclear heating, a 30 neutron+12  $\gamma$ -ray group transport and activity cross section data library CLAW-IV [29] has been used.

CLAW-IV represents an extended version of the Los Alamos National Laboratory (LANL) cross section data library CLAW [30], has point cross section linearization and resonance reconstruction tolerance of 0.5%, and all microscopic cross sections are Doppler broadened to 300 K. The neutron cross sections are averaged over 30 energy groups using the Bondarenko [31] flux approximation with a fusion, fission,  $1/E$ , thermal weight function. The energy structure is such that it has 12, 9 and 9 neutron groups in the MeV, keV and

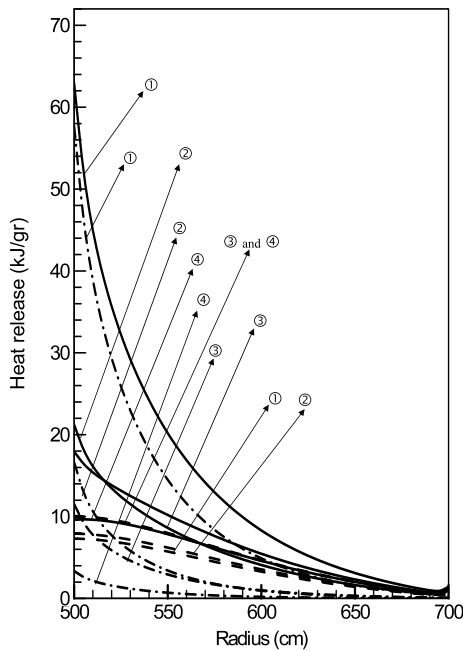


Fig. 10. Components of the nuclear power density vs. radius: (1): with 12%  $UF_4$  content; (2): with 12%  $ThF_4$  content; (3): with 2%  $UF_4$  content; (4): with 2%  $ThF_4$  content; —, total nuclear heating; - - - - -, (n, f) heating; - · - · - ·,  ${}^6Li(n, t){}^4He$  heating.

eV including thermal regions, respectively. The coupled 30 neutron+12  $\gamma$ -ray group data set includes also neutron induced secondary  $\gamma$ -rays. The heat production data has been processed under consideration of all energy producing nuclear reactions.

The transport calculations with the data library CLAW have been performed by solving the Boltzmann transport equation with the  $S_N$  transport code ANISN [28]. The contribution of  $\gamma$ -rays on total nuclear heating will grow in the presence of heavier elements. Especially, in mainline fusion reactor design concept, the metallic structures will be the major source of  $\gamma$ -ray heating. In the coolant zone of the PACER concept, there are no metals with the exception of fissionable isotopes. We have calculated the  $\gamma$ -ray heating for the lowest (2%) and highest (12%) uranium salt as he extreme cases.

Table 2 shows the integral heat production in the coolant for these compositions. One can notice that the  $\gamma$ -ray causes  $\sim 20\%$  of the induced nuclear heating in the coolant. As the main and primary energy source in a PNE reactor will be the PNE device itself, the  $\gamma$ -ray heating will constitute only a few% of the total plant energy generation. Compared with 238 group data library in SCALE4.4A, CLAW cross section set underestimates the nuclear heating. In a separate work, we have demonstrated the importance of high neutron energy group resolution as well as consideration of resonance self-shielding for each structure, individually [32]. Therefore, the 238 group data library is used throughout this study preferably.

#### 4.6. Neutron radiation damage

In the power plant, the only part exposed to nuclear radiation will be the steel liner at the periphery of the cavity, Fig. 3. All other components are totally separated from the nuclear zone. Beside thermo mechanical forces, the liner may suffer material damage under intense neutron radiation.

The displacement of an atom from its lattice position results from transferring a threshold energy, typically of the order of few dozens of electron volts, to the target. Atomic displacements

Table 2

Nuclear heat production in the coolant (in  $10^{-13}$  J/source fusion neutron)

Coolant type →	2% UF <sub>4</sub> –98% Li <sub>2</sub> - BeF <sub>4</sub>	12% UF <sub>4</sub> –88% Li <sub>2</sub> - BeF <sub>4</sub>
I	6.50	17.37
II	7.86 (17% $\gamma$ -ray)	22.05 (21% $\gamma$ -ray)
III	9.11	22.22

I: Neutron heat production calculated with 30 neutron groups (CLAW-IV). II: Neutron+ $\gamma$ -ray heat production calculated with 30 neutron groups+12  $\gamma$ -ray groups (CLAW-IV). III: Heat production calculated with 238 neutron groups (SCALE) according to equation (1).

are the fundamental process of radiation damage in metals. Calculations are conducted to determine, whether displacements of the atoms from their lattice sites as a result of collisions with highly energetic fusion neutrons can become a serious damage mechanism at the cavity liner.

At present there is non consensus about the damage limit criteria structural materials. Blink [33] suggests a DPA value of 165 for SS-316, though admitting that the DPA limit might be significantly higher than 165. The same limit is applied in [34]. A more conservative DPA value of 100 is assumed in [35,36]. Due to lack of experimental data, it is too early to state whether the actual DPA limit might be significantly higher than those. In an earlier work, DPA limits of the first-wall materials for MFE reactors and for IFE reactors were indicated as DPA = 300–1000 [37]. Only experiments conducted with an intense fusion neutron source can provide clarification about realistic damage limit data for advanced design work.

On the liner, we have calculated DPA values between 1.3 and 1.4 at the liner after an operation time of 30 full power years for the investigated coolant mixture range. Hence, no displacement damage is expected to occur in the liner.

An other very serious damage mechanism for structural materials can become gas production in the metallic lattice resulting from diverse nuclear reactions, mainly through (n, p) and (n,  $\alpha$ ) and to some extent through (n, d) and (n, t) reactions above a certain threshold energy. Materials suffer

from embrittlement due to gas bubble formation even for fission applications, which is in general at lower MeV range. The hydrogen isotopes will diffuse out of the metallic lattice under high operation temperatures, but  $\alpha$ -particle's will remain in metal and generate helium gas bubbles. These reactions may limit the lifetime of the liner. Blink and Perlado et al. [33,34] suggest a helium limit of 500 appm in steel. We have calculated helium production values below 7 and 4 ppm at the liner after an operation time of 30 full power years. Helium gas production will not cause a material damage at the liner during the life time of the plant.

## 5. Conclusions

The study has been conducted to assess the potential of the PACER concept for FFB in addition to electricity generation. It turns out that a PNE reactor can breed high quality nuclear fuel with extreme isotopic purity while producing energy.

Only a few mol.% of heavy metal in the molten salt will produce sufficient fissile fuel for the fission trigger of the PNE device. A Flibe coolant with up to 5 mol.% ThF<sub>4</sub> or with up to 9 mol.% UF<sub>4</sub> will allow a self-sufficient tritium breeding by a thickness of 2 m and with 25% liquid density in the jet zone. Heavy metal will be needed for an absolutely nuclear fuel independent operation of the PNE plant. Excess fissile fuel will be suitable for spacecraft applications or for other compact nuclear reactors.

Molybdenum is the main source for post shut down activity in steel structure of a fusion plant [15]. Use of SS-304 stainless steel without molybdenum constituent instead of SS-316 stainless steel in the absence of water coolant eliminates all residual radio activity originating from this material [17]. Low activation of the steel liner after 30 year of operation, satisfying the US Nuclear Regulatory Commission's rules for "shallow burial" upon decommissioning, assuming other sources of radioactivity could be removed or qualified as well, would make further utilization

the site possible. The cavity could be used as a shallow burial site for other qualified materials.

On the other hand, a PNE power plant is of highly prolific nature. The site with all nuclear peripheral sections, including explosive device manufacturing, power plant and fuel reprocessing must be sealed hermetically against nuclear diversion. Careful international nuclear safeguarding will be required.

## Acknowledgements

This work has been supported by the Research Fund of the Gazi University, Projects # 07/2001-15; 2003-14 and DPT-2003K 120470-08.

## References

- [1] Engineering with Nuclear Explosives, Proceedings of Third Plowshare Symposium, TID-7695, US Department of Energy/Office of Scientific and Technical Information, Oak Ridge, TN, 1964.
- [2] E. Teller, W. Talley, G. Higgins, Constructive Uses of Nuclear Explosives, McGraw-Hill Book Company, New York, 1968.
- [3] H.W. Hubbard, Project PACER Final Report, RDA-TR-4100-003, R&D Associates, 1974.
- [4] R.P. Hammond, Practical fusion power, Mech. Eng. 104 (1982) 34.
- [5] W. Seifritz, PACER: a ground design for fusion power, Fusion 4 (1980) 22.
- [6] R.W. Moir, PACER revisited, Fusion Technol. 15 (1989) 1114.
- [7] C.J. Call, R.W. Moir, A novel fusion power concept based on molten-salt technology: PACER revisited, Nucl. Sci. Eng. 104 (1990) 364.
- [8] A. Szöke, R.W. Moir, A practical route to fusion power, Technol. Rev. 94 (1991) 20.
- [9] A. Szöke, R.W. Moir, A realistic, gradual and economical approach to fusion power, Fusion Technol. 20 (1991) 1012.
- [10] R.P. Hammond, Practical fusion power, Mech. Eng. 104 (1982) 34.
- [11] H.W. Hubbard, Project PACER Final Report, R&D Associates, Santa Monica, CA, RDA-TR-4100-003, 1974.
- [12] V. David, A mechanical decoupling of underground nuclear explosion shock waves from the explosion cavity walls, Trans. Am. Nucl. Soc. 56 (1988) 127.
- [13] S. Şahin, R.W. Moir, J.D. Lee, S. Ünalán, Neutronic investigation of IFE blankets for HYLFE-II and MHD applications, Fusion Technol. 25 (1994) 388.

- [14] S. Şahin, R.W. Moir, S. Ünalán, Neutronic investigation of a power plant using peaceful nuclear explosives, *Fusion Technol.* 26 (1994) 1311.
- [15] S. Şahin, R.W. Moir, A. Şahinaslan, H.M. Şahin, Radiation damage in liquid-protected first wall materials for IFE-reactors, *Fusion Technol.* 30 (1996) 1027.
- [16] S. Şahin, A. Şahinaslan, M. Kaya, S. Yılmaz, Radiation Damage in Liquid-Protected First-Wall Materials for MFE-Reactors, *Transactions of the American Nuclear Society 1997 Winter Meeting*, 77 (16–20 November 1997) 158 (Albuquerque).
- [17] J.D. Lee, Waste disposal assessment of HYLIFE-II structure, *Fusion Technol.* 26 (1994) 74.
- [18] Licensing Requirements for Land Disposal of Radioactive Waste, Code of Federal Regulations, Title 10, Part 61 (1982).
- [19] S. Şahin, Examination of the radiation protection capability of different types of battle tanks against neutron bomb, *Bull. Technical Univ. İstanbul* 40 (1987) 315.
- [20] N.M. Greene, L.M. Petrie, XSDRNPM, A One-Dimensional Discrete-Ordinates Code For Transport Analysis, NUREG/CR-0200, Revision 5, vol. 2, Section F3, ORNL/NUREG/CSD-2/V2/R5, Oak Ridge National Laboratory, 1997.
- [21] S. Şahin, Radiation Shielding Calculations for Fast Reactors (in Turkish), Faculty of Science and Literature, Gazi University, Publication # 169, Publication number 22, Ankara, Turkey.
- [22] W.C. Jordan, S.M. Bowman, Scale Cross-Section Libraries, NUREG/CR-0200, Revision 5, vol. 3, section M4, ORNL/NUREG/CSD-2/V3/R5, Oak Ridge National Laboratory, 1997.
- [23] N.M. Greene, BONAMI, Resonance Self-Shielding by the Bondarenko Method, NUREG/CR-0200, Revision 5, vol. 2, section F1, ORNL/NUREG/CSD-2/V2/R5, Oak Ridge National Laboratory, 1997.
- [24] N.M. Greene, L.M. Petrie, R.M. Westfall, NITAWL-II, Scale System Module For Performing Resonance Shielding and Working Library Production, NUREG/CR-0200, Revision 5, vol. 2, Section F2, ORNL/NUREG/CSD-2/V2/R5, Oak Ridge National Laboratory, 1997b.
- [25] N.F. Landers, L.M. Petrie, CSAS, Control Module For Enhanced Criticality Safety Analysis Sequences, NUREG/CR-0200, Revision 5, vol. 1, Section C4, ORNL/NUREG/CSD-2/V1/R5, Oak Ridge National Laboratory, 1997.
- [26] S. Şahin, B. Şarer, Assessment of the neutron leakage spectrum of an enhanced radiation warhead for application as peaceful nuclear explosive, *Kerntechnik* 58 (1993) 295.
- [27] S. Şahin, R.W. Moir, S. Ünalán, Neutronic investigation of a power plant using peaceful nuclear explosives, *Fusion Technol.* 26 (1994) 1311.
- [28] W.W. Engle, Jr, ANISN, A One-Dimensional Discrete Ordinates Transport Code with Anisotropic Scattering, K1693, Oak Ridge National Laboratory, 1970.
- [29] T.A. Al-Kusayer, S. Şahin, A. Drira, CLAW-IV, Coupled 30 Neutrons, 12 Gamma Ray Group Cross Sections with Retrieval Programs for Radiation Transport Calculations, RSIC Newsletter, Radiation Shielding Information Center, Oak Ridge National Laboratory, May 1988, p. 4.
- [30] R.J. Barrett, R.E. Macfarlane, CLAW, Coupled 30 Neutrons, 12 Gamma-Ray Group Cross Sections for Neutron Transport Calculations, LA-7808-MS, Los Alamos Scientific Laboratory, 1979.
- [31] I.I. Bondarenko (Ed.), Group Constants for Nuclear Reactor Calculations, Consultants Bureau, New York, 1964.
- [32] S. Şahin, H.M. Şahin, K. Yıldız, Investigation of the Effects of the Resonance Absorption in a Fusion Breeder Blanket, *Annals of Nuclear Energy* 29 (2002) 1641.
- [33] A. Blink, in: K.L. Essary, K.E. Lewis (Eds.), High-Yield Lithium-Injection Fusion-Energy (HYLIFE) Reactor, UCRL-53559, Lawrence Livermore National Laboratory, 1985.
- [34] M. Perlado, M.W. Guinan, K. Abe, Radiation Damage in Structural Materials, Energy from Inertial Fusion, International Atomic Energy Agency, Vienna, 1995, p. 272.
- [35] R.W. Moir, HYLIFE-II, a molten-salt inertial fusion energy power plant design—final report, *Fusion Technol.* 25 (1994) 5.
- [36] D.L. Smith, Blanket Comparison and Selection Study—Final Report, ANL/FPP-84-1, Argonne National Laboratory, 1984.
- [37] J.J. Duderstad, G.A. Moses, Inertial Confinement Fusion, Wiley, New York, 1982, p. 315.